中正嶺學報 第三十二卷 第一期 民國 92.11
JOURNAL OF C.C.I.T. VOL.32 NO.1 Nov. 2003

短文 Short Paper

Algorithms for QAM Signal Classification Using Maximum Likelihood Approach Based on the Joint Probability Densities of Phases and Amplitudes

Yawpo Yang*, Jen-Ning Chang, Ji-Chyun Liu**, and Ching-Hwa Liu***

**Department of Electronics Engineering, China Institute of Technology*
***Department of Electrical Engineering, Chung Cheng Institute of Technology, National Defense University*

ABSTRACT

In this paper, we proposed three maximum likelihood-based algorithms for classifying the modulation type of M-ary QAM signals. Firstly, we derived the required test statistics and developed three classifiers for QAM signal classification based on the probability density functions (PDF) of amplitudes and phases of received signals. Secondly, We manifested the structures of the proposed classifier, analyzed and compared their performances in terms of the probability of successful classification using both theoretical analysis and computer simulations. In addition, we also compared with the classifier proposed by Yang *et al* [1]. Results indicate that the classifier based on the joint PDF is superior in performance to other classifiers and works very well even in low signal-to-noise ratio environment. Furthermore, the performances of all the classifiers are shown to be proportional to the number of samples and signal-to-noise ratios.

***Key Words*:** QAM, signal classification, maximum likelihood

基於相位及振幅聯合機率密度函數之最大概似 QAM 訊號調變型態分類演算法

楊耀波*　張振寧　劉智群**　劉慶華***

*中華技術學院電子系
**國防大學中正理工學院電機系

摘要

本論文提出最大概似函數為基礎之 M 準位正交振幅調變(M-ary QAM)型態分類法則。首先，依據接收訊號的振幅和相位及其聯合機率密度函數，我們推導三種測試統計並且據之發展三種 QAM 分類器。其次，我們說明所提出之分類器架構，接著經由理論探討與計算機模擬，分析、比較這三種分類器的性能。此外，本論文所提出之分類器也同時與由 Yang[1]等人所提的分類器進行性能比較。研究結果顯示，以聯合機率密度函數為基礎所發展之分類器，其性能較另二者為佳，尤其在低訊雜比的環境中仍具有相當優異的性能表現。此外，結果也指出，分類器性能跟樣本數目的多寡和接收訊號之訊雜比大小有直接的關係。

關鍵詞：正交振幅調變，調變型態分類，概似函數

文稿收件日期 91.10.26；文稿修正後以短文接受日期 92.6.16.

Manuscript received Oct. 26, 2002; revised as short paper June 16, 2003.

I. INTRODUCTION

Modulation classification is a specific area in the field of communication theory. In cooperative communication theory, almost of parameters involved detection at the receiver end are supposed to be known a priori or are accessible. In a general receiver, the parameters including modulation type, carrier frequency, bandwidth, symbol rate, carrier phase, etc. therefore, the received signal can be demodulated without ambiguity and then the data can be extracted. Modulation classification, which is used to recognize the modulation type of a received signal, however, is another story. Intrinsically, modulation classifier has not too much information about the signal emitter, and modulation classification is generally invisible to the signal emitter and is used as a means to pick up some useful information for either military or civic applications. For example, in military applications, modulation classification can be employed for electronic surveillance, interference identification, monitoring; in civic applications, it can be used for spectrum management, network traffic administration, different data rate allocation, etc. The criterion of performance of receiver in digital communication systems is usually the bit error probability; in the meanwhile, the criterion for modulation classification is the probability of correct classification [1-4].

A great number of techniques have been proposed to distinguish the specific modulation type from others within a record of received signal; the parameters adopted may be in the frequency domain or in the time domain, for examples, instantaneous frequency, instantaneous phase, envelopes, histogram, zero-crossing, moment, etc [1]. Generally, modulation classification schemes can be categorized in two approaches, namely, the statistical pattern recognition and the decision theoretic (or likelihood function) approaches. In decision theoretic approach, probabilistic and hypothesis testing arguments are used to formulate the classification problem and then the classification rule can be derived. The solution is usually optimal in the sense that it minimizes the error-rate classification. The disadvantage of this approach lies in that some knowledge must be available *a priori*. On the other hand, the statistical pattern recognition approach consists of two subsystems: the feature extraction subsystem and pattern recognition subsystem. The former is used to extract the useful information from the received signal, and the latter is employed to indicate the membership of modulation type. For this approach, training process is needed in the development stage.

Early researches on modulation schemes were concentrated on amplitude modulation (AM), frequency modulation (FM) of analog modulations, and M-ary amplitude-shift keying (MASK), M-ary phase-shift keying (MPSK), M-ary frequency-shift keying (MFSK) of digital modulations [1,5]. Recently another modulation scheme, quadrature amplitude modulation (QAM) has drawn a lot attention in the modulation classification research [2,5,6]. This is due to the fact that QAM's are frequently employed in digital microwave communications for high-speed transmission, in mobile communications, in telephone-line modems, for example, V.29, V.32, V.33, and V.34, and internet access such as ISDN, ADSL and HDSL.

In [1], Yang *et al.* applied the technique from maximum-likelihood decision theory to classify QAM signals buried in the additive white Gaussian noise (AWGN). Authors derived the log-likelihood functions based on the probability density function (PDF) of amplitudes and the classification rules were constructed. In [2], Schreyogg *et al.* applied the discrete Fourier transform (DFT) of phase histogram and distribution of amplitudes to recognize the PSK and QAM signals; the former is used to classify PSK signals, while the latter is used to classify QAM constellations. In [5], Sills classified PSK and QAM signals based on the PDF of I/Q component under coherent condition and on the PDF of amplitude and phase difference under noncoherent condition. In [3], W. Wei *et al.* also applied the maximum-likelihood method based on PDF of I/Q component to develop a generic classifier for classifying PAM and QAM signals. In [4], Taira extended the classification algorithm proposed by Yang *et al.* [1] to faded signals in the mobile fading channel.

In general, the rate of correct classification in virtue of likelihood function associated with two or more signal parameters, which offers more information about modulation type, is usually better than that obtained from individual likelihood function. The increased complexity is a chief cost for the multiple signal parameters. Since M-ary QAM signal is intrinsically a two-dimensional signal, QAM signals associated with different symbol levels (i.e., different M) have distinct constellations in signal space, which turn out to be different amplitude and phase sets. Accordingly, the prospective classification can be developed by utilizing the PDF of amplitudes or phases separately like [1,2,4] or jointly like [3,5]. As mentioned above, joint PDF of amplitudes and phases is expected to perform better.

In this paper, we extended the result in [1] to develop a more efficient classification algorithm to classify QAM signals by utilizing the complete information inherited in the QAM signal, namely the joint PDF of phase and amplitude of the signals. Signal representation in amplitude-phase plane has more advantageous than that in I/Q plane because in the amplitude-phase plane the characteristics of the signal can be exhibited directly. For example, the amplitudes and phases of the signals may be distorted jointly or separately in diverse fading channel.

This paper is organized as follows. In Section 2, we derive the three PDFs of M-ary QAM signals, which are the joint PDF of amplitudes and phases, the PDF of phases, and the PDF of amplitudes. In Section 3, we formulate the test statistics based on the three PDFs by using the maximum a posteriori probability criterion and then it turns out to be maximum likelihood style when all the hypotheses are assumed equally likely. Furthermore, we demonstrate a simplified structure to classify 16/32 QAM signals. In Section 4, we examine the performance of classifier by theoretical analysis and Monte Carlo computer simulations; the results illustrate that both approaches are closely accordant. Finally, in Section 5, we give a conclusion.

II. THE MODEL OF QAM SIGNALS IN AWGN CHANNEL

The received signal corrupted by AWGN in the interval $0 \le t \le T$ can be expressed as [7]

$$r(t) = s_m(t) + n(t), \quad 0 \le t \le T \tag{1}$$

where $s_m(t)$ denotes QAM signal waveforms and $n(t)$ denotes AWGN process with zero mean and covariance function $\sigma^2\delta(\tau)$ and is assumed to be uncorrelated with $s_m(t)$.

The QAM signal $s_m(t)$ is a bandpass signal and can be expressed in terms of the equivalent lowpass representation as

$$\begin{aligned} s_m(t) &= A_{mc}g(t)\cos 2\pi f_c t \\ &\quad - A_{ms}g(t)\sin 2\pi f_c t \\ &= \mathrm{Re}[s_{ml}(t)e^{j2\pi f_c t}] \\ &= A_m g(t)\cos(2\pi f_c t + \theta_m), \\ &\qquad m = 1,2,...M, \quad 0 \le t \le T \end{aligned} \tag{2}$$

where A_{mc} and A_{ms} are the information-bearing signal amplitudes of in-phase and the quadrature carriers respectively, $g(t)$ is the signal pulse shape, and f_c is the carrier frequency. $s_{ml}(t)$ is the complex envelope of $s_m(t)$. $A_m = \sqrt{A_{mc}^2 + A_{ms}^2}$ and $\theta_m = \tan^{-1}(A_{ms}/A_{mc})$. From this expression, it is apparent that the QAM signal waveforms may be viewed as combined amplitude and phase modulation. Note that the energy in $s_{ml}(t)$ is twice as much as that in $s_m(t)$ [7].

In a same manner, $n(t)$ can be represented in terms of its equivalent lowpass representation as

$$\begin{aligned} n(t) &= n_c(t)\cos 2\pi f_c t - n_s(t)\sin 2\pi f_c t \\ &= \mathrm{Re}[n_l(t)e^{j2\pi f_c t}] \end{aligned} \tag{3}$$

where $n_c(t)$ and $n_s(t)$ are in phase and the quadrature components of $n(t)$, $n_l(t)$ is the complex envelope of $n(t)$.

Hence, the received signal may be expressed as

$$\begin{aligned} r(t) &= s_m(t) + n(t) \\ &= (A_m g(t)\cos\theta_m + n_c(t))\cos 2\pi f_c t \\ &\quad - (A_m g(t)\sin\theta_m + n_s(t))\sin 2\pi f_c t, \\ &0 \le t \le T \end{aligned} \tag{4}$$

The envelope of $r(t)$ is [8]

$$z(t) = \sqrt{z_c^2(t) + z_s^2(t)} \tag{5}$$

where $z_c(t) = A_m g(t)\cos\theta_m + n_c(t)$ and $z_s(t) = A_m g(t)\sin\theta_m + n_s(t)$.

For any given value of θ_m and the pulse shape $g(t) = 1, 0 \le t \le T$, both $z_c(t)$ and $z_s(t)$ are Gaussian processes and may be shown to be uncorrelated, henceforth statistically independent [8]. The means and variances of $z_c(t)$ and $z_s(t)$ can be expressed as

$$\begin{aligned} E[z_c(t)] &= A_m \cos\theta_m \\ E[z_s(t)] &= A_m \sin\theta_m \end{aligned} \tag{6}$$

$$V[z_c(t)] = V[z_s(t)] = \sigma^2 \tag{7}$$

where $E[\cdot]$, $V[\cdot]$ denote the mean and variance, respectively, of the random variable in the brackets following.

At the same time instant, and $z_c(t)$ and $z_s(t)$ can be in terms of z_c and z_s, respectively. Thus the joint PDF of z_c and z_s is [8]

$$\begin{aligned} p(z_c, z_s) &= \frac{1}{2\pi\sigma^2} \\ &\quad \cdot e^{-\frac{1}{2\sigma^2}[(z_c - A_m\cos\theta_m)^2 + (z_s - A_m\sin\theta_m)^2]} \end{aligned} \tag{8}$$

By making changes in variables as $z_c = z\cos\varphi$ and $z_s = z\sin\varphi$, the envelope of $r(t)$ is then

$$z = \sqrt{z_c^2 + z_s^2}, \quad z \ge 0 \tag{9}$$

and the phase of $r(t)$ is

$$\varphi = \tan^{-1}(z_s / z_c), \quad -\pi < \varphi \le \pi \tag{10}$$

Consequently, the joint PDF of amplitudes and phases can be written as [7]

$$p(z,\varphi) = \frac{z}{2\pi\sigma^2} e^{-\frac{z^2 + A_m^2 - 2A_m z\cos(\theta_m - \varphi)}{2\sigma^2}} \tag{11}$$

and the integration of $p(z,\varphi)$ over the range of φ yields the amplitude PDF $p(z)$. That is

$$\begin{aligned} p(z) &= \int_0^{2\pi} p(z,\varphi)d\varphi \\ &= \frac{z}{\sigma^2} e^{-\frac{1}{2\sigma^2}(z^2 + A_m^2)} I_0\left(\frac{A_m z}{\sigma^2}\right) \end{aligned} \tag{12}$$

where $I_0(\cdot)$ is the modified Bessel function of the first kind with zero order.

Note that the PDF of z is independent of θ_m, and so is the PDF of envelope of $r(t)$, and the resulting PDF is referred to the Rice distribution.

Similarly, the PDF of phase φ can be obtained as

$$\begin{aligned} &p(\varphi) \\ &= \int_0^{\infty} p(z,\varphi)dz \\ &= \frac{e^{-\frac{A_m^2}{2\sigma^2}}}{2\pi} + \frac{A_m\cos(\theta_m - \varphi)}{\sqrt{2\pi}\sigma} \\ &\quad \cdot e^{-\frac{A_m^2}{2\sigma^2}\sin^2(\theta_m - \varphi)} Q\left[-\frac{A_m}{\sigma}\cos(\theta_m - \varphi)\right], \\ &\quad -\pi < \varphi \le \pi \end{aligned} \tag{13}$$

where $Q(x) = \frac{1}{\sqrt{2\pi}}\int_x^{\infty} e^{-t^2/2}dt, \quad x \ge 0$

Constellations of M-ary QAM signals may be circular and rectangular; however, the rectangular QAM signal constellations are easily generated and demodulated, and the average transmitted power required to achieve a given bit error probability is only slightly greater than the average power require for the best QAM signal constellation. For these reasons, rectangular QAM signals are frequently used in practice [7]. Hence, the rectangular QAM signals will be dealt with in this paper.

A. Representation of the Joint PDF of Amplitudes and Phases of M-ary QAM Signal

Suppose that the *m*th message point for M-ary QAM signal is represented by amplitude A_m and phase θ_m. Following Eq. (11), the joint PDF of amplitudes and phases of M-ary QAM can be expressed as

$$p_M(z,\varphi)=\frac{1}{M}\sum_{m=1}^{M}\frac{z}{2\pi\sigma^2}\cdot e^{-\frac{z^2+A_{M,m}^2-2A_{M,m}z\cos(\theta_{M,m}-\varphi)}{2\sigma^2}} \tag{14}$$

where $A_{M,m}$, $\theta_{M,m}$ represent the amplitude and phase of the *m*th message point of an M-ary QAM signal respectively.

For example, for a 16QAM signal the joint PDF of amplitudes and phases is

$$p_{16}(z,\varphi)=\frac{1}{16}\sum_{m=1}^{16}\frac{z}{2\pi\sigma^2}\cdot e^{-\frac{z^2+A_{16,m}^2-2A_{16,m}z\cos(\theta_{16,m}-\varphi)}{2\sigma^2}} \tag{15}$$

Let A be the minimum amplitude among the message points, then the pairs $A_{16,m}$ and $\theta_{16,m}$ can be expressed in terms of *A*, and phases $\theta_{16,1}$ represents the minimum phase and $\theta_{16,16}$ the maximum phase. The set of amplitudes and phases can be written as

$$\begin{aligned}\{\mathbf{A}_{M,m},\boldsymbol{\theta}_{M,m}\}&=\{\{A_{16,1},\theta_{16,1}\},\ldots,\{A_{16,16},\theta_{16,16}\}\}\\&=\{\{\sqrt{5}A,\tan^{-1}[1/3]\},\{A,\pi/4\},\\&\quad\{3A,\pi/4\},\{\sqrt{5}A,\tan^{-1}[3]\},\\&\quad\{\sqrt{5}A\tan^{-1}[3]+\pi/2\},\{A,3\pi/4\},\\&\quad\{3A,3\pi/4\},\{\sqrt{5}A,\tan^{-1}[1/3]+\pi/2\},\\&\quad\{\sqrt{5}A,\tan^{-1}[1/3]+\pi\},\{A,5\pi/4\},\\&\quad\{3A,5\pi/4\},\{\sqrt{5}A,\tan^{-1}[3]+\pi\},\\&\quad\{\sqrt{5}A,\tan^{-1}[3]+3\pi/2\},\{A,7\pi/4\},\\&\quad\{3A,7\pi/4\},\{\sqrt{5}A,\tan^{-1}[1/3]+3\pi/2\}\}\end{aligned} \tag{16}$$

Plots of the joint PDF of amplitudes and phases of M-ary QAM signals at SNR=20 dB are illustrated. In Fig. 1 is the 16QAM signal with $A=\sqrt{40}=6.3246$, and in Fig. 2 is the 32QAM signal with $A=\sqrt{20}=4.4721$

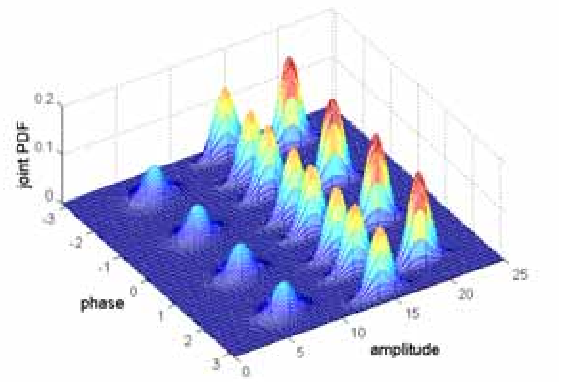

Fig.1. The joint PDF of amplitudes and phases of 16QAM signal at SNR=20dB.

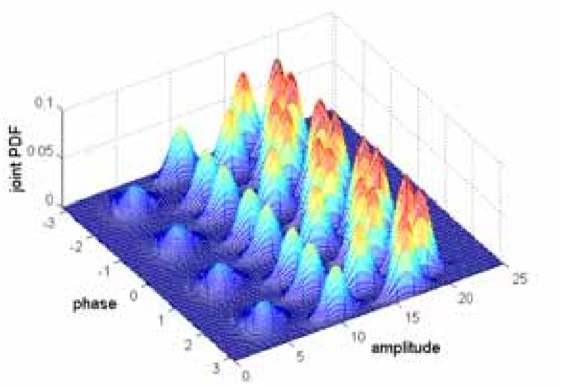

Fig.2. The joint PDF of amplitudes and phases of 32QAM signal at SNR=20dB.

B. The amplitude PDF of QAM signal

The amplitude PDF of M-ary QAM signals can be represented from Eq.(12) as

$$p_M(z)=\frac{4}{M}\sum_{m=1}^{M/4}\frac{z}{\sigma^2}e^{-\frac{1}{2\sigma^2}(z^2+A_{M,m}^2)}\cdot I_0\left(\frac{A_{M,m}z}{\sigma^2}\right),\quad z\ge 0 \tag{17}$$

For example, the amplitude PDFs of 16QAM and 32QAM at SNR=20 dB are plotted in Fig. 3 and Fig. 4 respectively, where $A=\sqrt{40}=6.3246$ for 16QAM and $A=\sqrt{20}=4.4721$ for 32QAM.

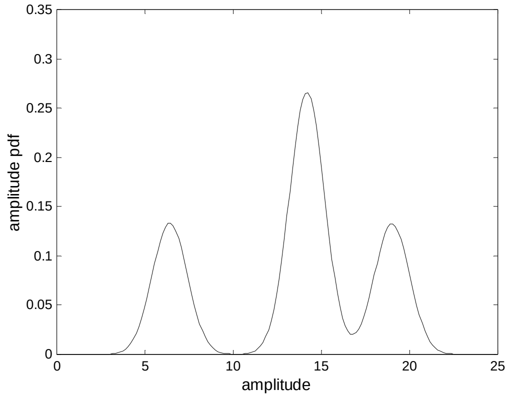

Fig.3. The amplitude PDF of 16QAM at SNR=20dB.

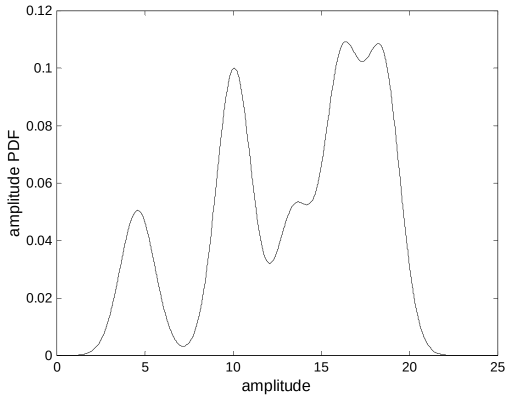

Fig.4. The amplitude PDF of 32QAM at SNR=20dB.

C. The Phase PDF of QAM Signal

For M-ary QAM signals, it can be shown that $\theta_{M,m}$ is periodic with period $\pi/2$, consequently, the phases can be denoted by $\theta_{M,m}$, $m=1,2,\ldots,M/4$. The phase PDF of M-ary QAM signals can be derived from Eq. (13) and can be written as

$$\begin{aligned} & p_M(\varphi) \\ & = \frac{4}{M}\sum_{m=1}^{M/4}\{\frac{e^{-\frac{A_{M,m}^2}{2\sigma^2}}}{2\pi}+\frac{A_{M,m}\cos(\theta_{M,m}-\varphi)}{\sqrt{2\pi}\sigma} \\ & e^{-\frac{A_{M,m}^2}{2\sigma^2}\sin^2(\theta_{M,m}-\varphi)} Q[-\frac{A_{M,m}}{\sigma}\cos(\theta_{M,m}-\varphi)]\}, \\ & \qquad 0 \le \varphi \le \pi/2 \end{aligned} \tag{18}$$

The phase PDFs of 16QAM and 32QAM at SNR=20 dB are illustrated in Fig. 5 and Fig. 6.

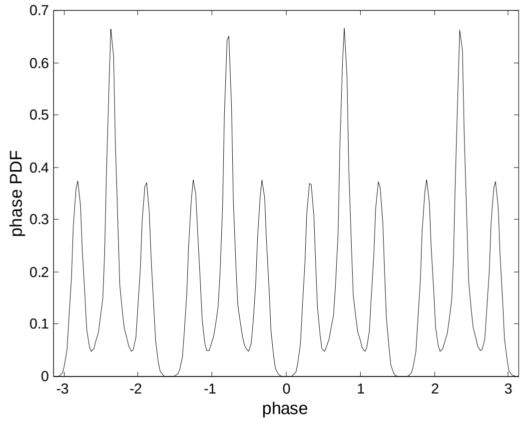

Fig.5. The phase PDF of 16QAM at SNR=20dB.

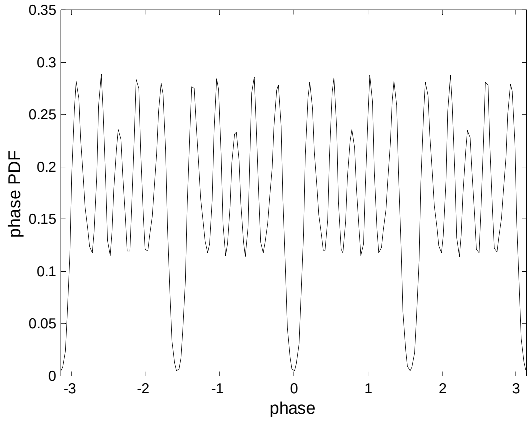

Fig.6. The phase PDF of 32QAM at SNR=20dB.

III. LOG-LIKELIHOOD FUNCTION BASED QAM CLASSIFICATION RULES

Once the transmitted signal corrupted by AWGN is received, the detector at the receiver end can yield the vector $\mathbf{r}=[r_1\ r_2\ ...\ r_N]$, where N is the number of samples in a symbol interval. The vector $\mathbf{r}$ contains all the relevant information in the received signal waveform [7]. In the section, we develop the decision rule by employing the intrinsic information in the vector $\mathbf{r}$ and demonstrate a classifier to classify which of the M possible signal waveforms was transmitted.

In development of such classification algorithm, we formulate the classification problem as a hypotheses problem, that is, an L-hypothesis test problem which is written as:

$$\begin{aligned} H_\alpha:\quad & r_i = s_{mi}+n_i, \quad \alpha=1,2,...,L, \\ & i=1,2,...,N, \quad m=1,2,...,M \end{aligned} \tag{19}$$

where $L=\log_2[M]-3$ and r_i, s_{mi}, and n_i are, respectively, the sampled data from the ith symbol interval $iT\le t\le(i+1)T$ of $r(t)$, $s_m(t)$ and $n(t)$. The samples n_i are assumed independent; therefore, independent and identically distribution (i.i.d.).

The decision rule can be obtained by choosing the largest among the L hypotheses. If we express the posterior probabilities as

$$P(H_\alpha\,|\,\mathbf{r}) \tag{20}$$

then the decision rule is corresponding to choose the maximum of the set of posterior probabilities $\{P(H_\alpha\,|\,\mathbf{r})\}$. This criterion is called the maximum a posteriori probability (MAP). In other words, the decision rule is to choose H_α if

$$P(H_\alpha\,|\,\mathbf{r}) > P(H_\beta\,|\,\mathbf{r}) \tag{21}$$

Using Bayes' rules, the posterior probabilities can be expressed as

$$P(H_\alpha\,|\,\mathbf{r}) = \frac{p(\mathbf{r}\,|\,H_\alpha)P(H_\alpha)}{p(\mathbf{r})} \tag{22}$$

where $p(\mathbf{r}\,|\,H_\alpha)$ is the conditional PDF of the observed vector under hypothesis H_α, and $P(H_\alpha)$ is the *a priori* probability of hypothesis H_α, $\alpha=1,2,...,L$. From Eq. (22), we observe that the computation of the posterior probabilities $P(H_\alpha\,|\,\mathbf{r})$ requires knowledge of the *a priori* probabilities $P(H_\alpha)$ and the conditional PDFs $p(\mathbf{r}\,|\,H_\alpha)$, but $p(\mathbf{r})$ is independent of H_α and can be neglected.

The *a priori* probabilities $P(H_\alpha)$ are assumed equally likely without loss of generality. As a result, the decision rule based on the maximum of $P(H_\alpha\,|\,\mathbf{r})$ is equivalent to finding the signal that maximizes $p(\mathbf{r}\,|\,H_\alpha)$ Such criterion is called the maximum-likelihood (ML) and the conditional PDF $p(\mathbf{r}\,|\,H_\alpha)$ is called the likelihood function or decision function.

Since the noise samples n_i are assumed to be i.i.d., the conditional PDF of the random vector $\mathbf{r}$ is the product of N individual PDF's as

$$\begin{aligned} p(\mathbf{r}|H_\alpha) &= p(r_1,r_2,...,r_N\,|\,H_\alpha) \\ &= \prod_{i=1}^{N} p(r_i\,|\,H_\alpha) \end{aligned} \tag{23}$$

To simplify the computations and from the fact that the natural logarithm function $\ln(x)$ is a monotonic function of x, we may take the natural logarithm of $p(\mathbf{r}\,|\,H_\alpha)$. The resulting log likelihood function or called the test statistic of hypothesis H_α, l_α, is expressed by

$$\begin{aligned} l_\alpha &= \ln[p(\mathbf{r}\,|\,H_\alpha)] \\ &= \sum_{i=1}^{N} \ln[p(r_i\,|\,H_\alpha)], \quad \alpha=1,2,...,L \end{aligned} \tag{24}$$

From Eq.(14), the test statistics for M-ary QAM signal associated with joint PDF of amplitudes and phases can be expressed as

$$
\begin{aligned}
l_{\alpha,\mathbf{z\varphi}} &= \ln[p(\mathbf{z},\boldsymbol{\varphi} \mid H_\alpha)] \\
&= \sum_{i=1}^{N} \ln[p_M(z_i,\varphi_i)] \\
&= \sum_{i=1}^{N} \ln[\sum_{m=1}^{M} \frac{z_i}{2\pi\sigma^2} \\
&\quad \cdot e^{-\frac{z_i^2 + A_{M,m}^2 - 2A_{M,m} z_i \cos(\theta_{M,m}-\varphi_i)}{2\sigma^2}}], \\
&\alpha = 1,2,\ldots,L, \quad M = 16,32,\ldots,2^{L+3}
\end{aligned} \qquad (25)
$$

where z_i and φ_i are amplitude and phase of r_i.

In a same manner, the test statistic for M-ary QAM signal associated with amplitude PDF can be expressed as

$$
\begin{aligned}
l_{\alpha,\mathbf{z}} &= \ln[p(\mathbf{z} \mid H_\alpha)] \\
&= \sum_{i=1}^{N} \ln[p_M(z_i)] \\
&= \sum_{i=1}^{N} \ln[\sum_{m=1}^{M} \frac{z_i}{\sigma^2} e^{-\frac{1}{2\sigma^2}(z_i^2 + A_{M,m}^2)} \cdot I_0(\frac{A_{M,m} z_i}{\sigma^2}), \\
&\alpha = 1,2,\ldots,L, \quad M = 16,32,\ldots,2^{L+3}
\end{aligned} \qquad (26)
$$

Similarly, the test statistic for M-ary QAM signal with phase PDF can be expressed as

$$
\begin{aligned}
& l_{\alpha,\boldsymbol{\varphi}} \\
&= \ln[p(\boldsymbol{\varphi} \mid H_\alpha)] \\
&= \sum_{i=1}^{N} \ln[p_M(\varphi_i)] \\
&= \sum_{i=1}^{N} \ln\{\sum_{m=1}^{M} \{\frac{e^{-\frac{A_{M,m}^2}{2\sigma^2}}}{2\pi} + \frac{A_{M,m}\cos(\theta_{M,m}-\varphi_i)}{\sqrt{2\pi}\sigma} \\
&\quad \cdot e^{-\frac{A_{M,m}^2}{2\sigma^2}\sin^2(\theta_{M,m}-\varphi_i)} Q[-\frac{A_{M,m}}{\sigma}\cos(\theta_{M,m}-\varphi_i)]\}\}, \\
&\alpha = 1,2,\ldots,L, \quad M = 16,32,\ldots,2^{L+3}
\end{aligned} \qquad (27)
$$

In the following we employ the test statistics of Eqs.(25), (26), and (27), which are based on different PDFs, to design three distinct classifiers respectively.

For example, Fig. 7 is the classifier based on the joint PDF of amplitudes and phases.

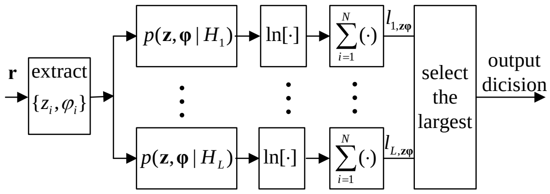

Fig.7. The structure of classifier based joint PDF of amplitude and phase

VI. PERFORMANCE ANALYSIS AND NUMERICAL RESULTS

In this section, we will analyze and compare the performance of the proposed classifiers, viz., the probability of successful classification. To evaluate the performance, we need to know the statistics of the decision function first. Unfortunately, they are too complex to obtain. As an alternative, approximation is usually employed to bypass this obstacle. By virtue of the central limit theorem, as N, the number of samples, is large enough, $l_{\alpha,\mathbf{z\varphi}}$, $l_{\alpha,\mathbf{z}}$ and $l_{\alpha,\boldsymbol{\varphi}}$ can be treated as Gaussian distributions. Accordingly, only mean and variance is enough to describe the statistics of log-likelihood function. For example, the mean and variance of $l_{\alpha,\mathbf{z\varphi}}$ can be expressed as

$$\mu_{\alpha,\mathbf{z\varphi}} = E[l_{\alpha,\mathbf{z\varphi}}] \qquad (28)$$

and

$$\sigma_{\alpha,\mathbf{z\varphi}}^2 = E[(l_{\alpha,\mathbf{z\varphi}} - \mu_{\alpha,\mathbf{z\varphi}})^2] \qquad (29)$$

where $\mu_{\alpha,\mathbf{z\varphi}}$ and $\sigma_{\alpha,\mathbf{z\varphi}}^2$ represent the ensemble mean and variance of test statistic $l_{\alpha,\mathbf{z\varphi}}$ when the input is a specific "M-ary" QAM signal to which H_α is assigned. Generally, it is difficult to find the closed-form expressions for $\mu_{\alpha,\mathbf{z\varphi}}$ and $\sigma_{\alpha,\mathbf{z\varphi}}^2$.

Here we demonstrate a classifier for 16/32QAM signals, which is obtained by simplifying the structures of Fig. 7.

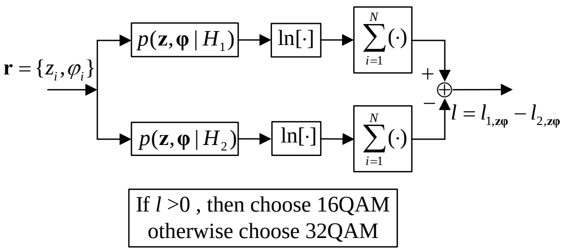

Fig.8. The structure of 16/32 QAM classifier based on joint PDF of amplitudes and phases.

The means and variances of these three test statistics may be computed in the similar manner. First, we analyze the performance of the classifier based joint PDF of amplitudes and phases. The ensemble mean can be calculated as

$$\begin{aligned}
&\mu_{\alpha,\mathbf{z\varphi}} \\
&= \underbrace{\int_0^{\infty}\cdots\int_0^{\infty}}_{N}\underbrace{\int_0^{\pi/2}\cdots\int_0^{\pi/2}}_{N} l p(\mathbf{z},\boldsymbol{\varphi}\,|\,H_\alpha)\,d\boldsymbol{\varphi}\,d\mathbf{z} \\
&= \underbrace{\int_0^{\infty}\cdots\int_0^{\infty}}_{N}\underbrace{\int_0^{\pi/2}\cdots\int_0^{\pi/2}}_{N} \qquad (30)\\
&\quad l p(z_1,\varphi_1\,|\,H_\alpha)\ldots p(z_N,\varphi_N\,|\,H_\alpha) \\
&\quad d\varphi_1\ldots d\varphi_N\,dz_1\ldots dz_N, \\
&\quad \alpha = 1,2,\ldots,L
\end{aligned}$$

where $l = \sum_{i=1}^{N}\ln[p_{16}(z_i,\varphi_i)] - \sum_{i=1}^{N}\ln[p_{32}(z_i,\varphi_i)]$.

Let $\ell = \ln[p_{16}(z,\varphi)] - \ln[p_{32}(z,\varphi)]$, and the ensemble means can be obtained as

$$\mu_{1,\mathbf{z\varphi}} = N\int_0^{\infty}\int_0^{\pi/2} \ell p_{16}(z,\varphi)\,d\varphi\,dz \qquad (31)$$

and

$$\mu_{2,\mathbf{z\varphi}} = N\int_0^{\infty}\int_0^{\pi/2} \ell p_{32}(z,\varphi)\,d\varphi\,dz \qquad (32)$$

The ensemble variances are as

$$\sigma_{1,\mathbf{z\varphi}}^2 = N\int_0^{\infty}\int_0^{\pi/2} (\ell - \frac{\mu_{1,\mathbf{z\varphi}}}{N})^2\, p_{16}(z,\varphi)\,d\varphi\,dz \qquad (33)$$

and

$$\sigma_{2,\mathbf{z\varphi}}^2 = N\int_0^{\infty}\int_0^{\pi/2} (\ell - \frac{\mu_{2,\mathbf{z\varphi}}}{N})^2\, p_{32}(z,\varphi)\,d\varphi\,dz \qquad (34)$$

The performance is the probability of the successful classification and can be expressed as

$$\begin{aligned}
P(sucess\,|\,H_1) &= \int_0^{\infty}\frac{1}{\sqrt{2\pi\sigma_{1,\mathbf{z\varphi}}^2}}e^{\frac{-(x-\mu_{1,\mathbf{z\varphi}})^2}{2\sigma_{1,\mathbf{z\varphi}}^2}}\,dx \\
&= \int_{-\frac{\mu_{1,\mathbf{z\varphi}}}{\sigma_{1,\mathbf{z\varphi}}}}^{\infty}\frac{1}{\sqrt{2\pi}}e^{-\frac{x^2}{2}}\,dx \qquad (35)\\
&= Q\left(-\frac{\mu_{1,\mathbf{z\varphi}}}{\sigma_{1,\mathbf{z\varphi}}}\right)
\end{aligned}$$

$$\begin{aligned}
P(sucess\,|\,H_2) &= \int_{-\infty}^{0}\frac{1}{\sqrt{2\pi\sigma_{2,\mathbf{z\varphi}}^2}}e^{\frac{-(x-\mu_{2,\mathbf{z\varphi}})^2}{2\sigma_{2,\mathbf{z\varphi}}^2}}\,dx \\
&= \int_{-\infty}^{-\frac{\mu_{2,\mathbf{z\varphi}}}{\sigma_{2,\mathbf{z\varphi}}}}\frac{1}{\sqrt{2\pi}}e^{-\frac{x^2}{2}}\,dx \qquad (36)\\
&= Q\left(\frac{\mu_{2,\mathbf{z\varphi}}}{\sigma_{2,\mathbf{z\varphi}}}\right)
\end{aligned}$$

where $Q(x) = \int_x^{\infty}\frac{1}{\sqrt{2\pi}}e^{-\frac{y^2}{2}}\,dy$.

The average probability of successful classification is then written as:

$$\begin{aligned}
&P(success) \\
&= \frac{P(success\,|\,H_1) + P(success\,|\,H_2)}{2} \qquad (37)\\
&= \frac{Q\left(-\frac{\mu_{1,\mathbf{z\varphi}}}{\sigma_{1,\mathbf{z\varphi}}}\right) + Q\left(\frac{\mu_{2,\mathbf{z\varphi}}}{\sigma_{2,\mathbf{z\varphi}}}\right)}{2}
\end{aligned}$$

The performance of classifiers based on $l_{\alpha,\mathbf{z}}$ and $l_{\alpha,\boldsymbol{\varphi}}$ can be evaluated using the same philosophy. The performance of three classifiers with theoretical analysis and Monte Carlo simulations is shown in Fig. 9.

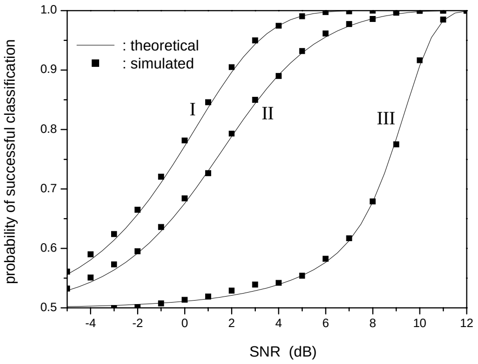

Fig.9. The performance of three distinct classifiers. Curve I represents the performance of the classifier based on the joint PDF of amplitudes and phases, curve II represents the performance of the classifier based on the phase PDF only, and curve III is based on the amplitude PDF only [1].

Monte Carlo simulations are carried out with the simulation tools: ACOLADE [10] (Advanced Communication Link Analysis and Design) and MATLAB with PC-based windows as platform.

Figure 9 shows that the results of both theoretical analysis and numerical simulation are almost consistent, where the number of samples is set to 1024. Inspecting Fig. 9, we observe that curve I always outperforms among three classifiers. For example, at 90% successful rate, the SNR needed with curve I is about 2 dB, but the SNR needed with curve II is about 4.5 dB, and is about 10 dB with curve III.

Another manifestation for performance is the probability of failure classification, which can be defined as

$$P(failure) = 1 - P(success) = \frac{Q\left(\frac{\mu_{1,\mathbf{z\varphi}}}{\sigma_{1,\mathbf{z\varphi}}}\right) + Q\left(-\frac{\mu_{2,\mathbf{z\varphi}}}{\sigma_{2,\mathbf{z\varphi}}}\right)}{2} \quad (38)$$

Figure 10 shows the performance of classifiers in terms of the probability of failure classification.

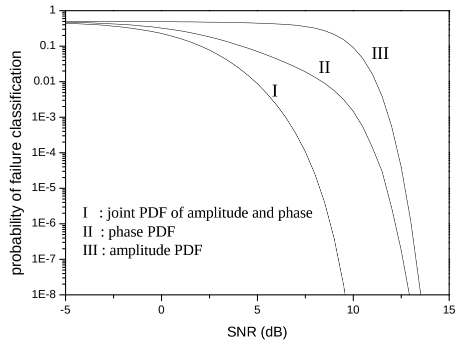

Fig.10. The probability of failure classification of classifiers.

It is worthy to note from Fig. 10 that the difference between curves II and III diminishes with the increase of SNR, which means that at high SNR, both classifiers perform almost the same.

From Eqs. (31), (32), (33), and (34), and by letting

$$\mu_{1,z\varphi} = \int_0^{\infty}\int_0^{\pi/2} \ell p_{16}(z,\varphi)dzd\varphi \quad (39)$$

$$\mu_{2,z\varphi} = \int_0^{\infty}\int_0^{\pi/2} \ell p_{32}(z,\varphi)dzd\varphi \quad (40)$$

$$\sigma_{1,z\varphi}^2 = \int_0^{\infty}\int_0^{\pi/2} (\ell - \mu_{1,z\varphi})^2 p_{16}(z,\varphi)dzd\varphi \quad (41)$$

and

$$\sigma_{2,z\varphi}^2 = \int_0^{\infty}\int_0^{\pi/2} (\ell - \mu_{2,z\varphi})^2 p_{32}(z,\varphi)dzd\varphi \quad (42)$$

We can obtain

$\mu_{1,\mathbf{z\varphi}} = N\mu_{1,z\varphi}$, $\mu_{2,\mathbf{z\varphi}} = N\mu_{2,z\varphi}$, $\sigma_{1,\mathbf{z\varphi}}^2 = N\sigma_{1,z\varphi}^2$,

and $\sigma_{2,\mathbf{z\varphi}}^2 = N\sigma_{2,z\varphi}^2$ (43)

Consequently, the average probability of successful classification can be expressed in terms of the Q function as,

$$P(success) = \frac{Q\left(-\frac{\mu_{1,z\varphi}}{\sigma_{1,z\varphi}}\right)+Q\left(\frac{\mu_{2,z\varphi}}{\sigma_{2,z\varphi}}\right)}{2} = \frac{Q\left(-\frac{\sqrt{N}\mu_{1,z\varphi}}{\sigma_{1,z\varphi}}\right)+Q\left(\frac{\sqrt{N}\mu_{2,z\varphi}}{\sigma_{2,z\varphi}}\right)}{2} \quad (44)$$

It is reasonable to expect that the performance will be better with the increase of the number of samples. Fig. 11 justifies this point and illustrates the relationship between the probability of successful classification and the number of samples.

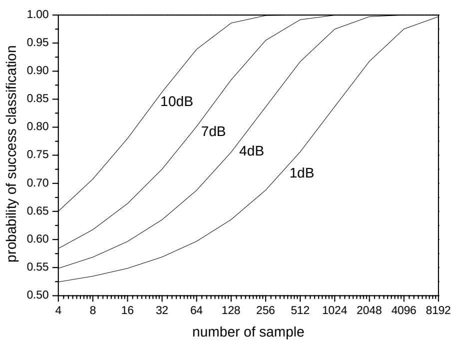

Fig.11. The performance based on joint PDF of amplitudes and phases as a function of the number of samples with SNR as parameter.

V. CONCLUSIONS

In this paper, we have developed the algorithms for classifying QAM signal buried in the AWGN. The algorithms are derived from three PDFs of amplitudes and phases extracted from the received signals with the maximum likelihood criterion. We have also demonstrated the performances of classifier in terms of the probability of successful classification. Among these proposed classification algorithms, we conclude that the classification algorithm based on the joint PDF of amplitudes and phases is superior to others and works very well even in low signal-to-noise ratio environment. Furthermore, the performances of all the classifiers are also proportional to the number of samples, signal-to-noise ratios.

REFERENCES

[1] Yang, Y., Liu, C. H., and Soong, T. W., "A Log-Likelihood Function-Based Algorithm for QAM signal classification," Signal Processing 70, pp. 61-71, 1998.

[2] Schreyogg, C. and Reichert, J. "Modulation Classification of QAM schemes Using the DFT of Phase Histogram Combined With Modulus Information," MILCOM97 Proc., Vol. 3, pp. 1372-1376, 1997.

[3] Wei, W. and Mendel, J. M., "Maximum-Likelihood Classification for Digital Amplitude-Phase Modulations, "IEEE Trans. on Commun. Vol. 48, No. 2, pp. 189-193, Feb. 2000.

[4] Taira, S. "Automatic Classification of QAM Signals in Fading Channel," VTC2000 Proc., Vol.3, pp. 1717-1721, 2000.

[5] Sills, J. A., "Maximum Likelihood Modulation Classification for PSK/QAM," MILCOM99, Proc., Vol. 1, pp.217-220, 1999.

[6] Benvenuto, N. and Goeddel, T. W., "Classification of Voiceband Data Signals Using the Constellation Magnitude," IEEE Trans. Commun., Vol. 43, No. 11, pp. 2759-2770, Nov. 1995.

[7] Proakis, J. G., Digital Communications, 4th ed., New York, McGraw-Hill, 2001.

[8] Whalen, A. D., Detection of Signals in Noise, Academic Press, New York, 1971.

[9] Van Tree, H. L., Detection, Estimation, and Modulation Theory, Part I, Wiley, New York, 1968.

[10] ICUCOM, ACOLADE User's Manual, ICUCOM Corp., Troy, New York, 1995.

[11] Papoulis, A., Probability, Random Variables, and Stochastic Processes, 3rd ed., McGraw-Hill, New York, 1991.